



Please cite the Published Version

Lau, Iain, Ekpo, Sunday , Zafar, Muazzam, Ijaz, Muhammad  and Gibson, Andrew (2023) Hybrid mmWave-Li-Fi 5G Architecture for Reconfigurable Variable Latency and Data Rate Communications. IEEE Access, 11. pp. 42850-42861. ISSN 2169-3536

DOI: <https://doi.org/10.1109/ACCESS.2023.3270777>

Publisher: IEEE

Version: Published Version

Downloaded from: <https://e-space.mmu.ac.uk/631796/>

Usage rights:  [Creative Commons: Attribution 4.0](https://creativecommons.org/licenses/by/4.0/)

Additional Information: This is an Open Access article that was published in IEEE Access.

Enquiries:

If you have questions about this document, contact openresearch@mmu.ac.uk. Please include the URL of the record in e-space. If you believe that your, or a third party's rights have been compromised through this document please see our Take Down policy (available from <https://www.mmu.ac.uk/library/using-the-library/policies-and-guidelines>)

Received 22 March 2023, accepted 19 April 2023, date of publication 26 April 2023, date of current version 4 May 2023.

Digital Object Identifier 10.1109/ACCESS.2023.3270777

RESEARCH ARTICLE

Hybrid mmWave-Li-Fi 5G Architecture for Reconfigurable Variable Latency and Data Rate Communications

IAIN LAU^{ID}, SUNDAY EKPO^{ID}, (Senior Member, IEEE), MUAZZAM ZAFAR, MUHAMMAD IJAZ^{ID}, (Member, IEEE), AND ANDY GIBSON

Department of Engineering, Manchester Metropolitan University, M15 6BH Manchester, U.K.

Corresponding author: Iain Lau (Iain.Lau@stu.mmu.ac.uk)

This work was supported in part by the Manchester Metropolitan University under the Innovation and Industrial Engagement Fund, and in part by the Smart Infrastructure and Industry Research Group's Open Bid Scheme.

ABSTRACT Despite modern vehicles having the necessary advanced driver assistance systems (ADAS) for autonomous operation, current implementations rely solely on sensor information from the surrounding environment or data from smart infrastructure. However, shortcomings in current implementations and standards around cost-effective variable latency and data rate have prevented widespread adoption of the technology to enable autonomous operations. This paper presents a proof-of-concept (PoC) reconfigurable design and performance of a hybrid ultra-high bands [i.e., millimetre-Wave (mmWave)-light fidelity (Li-Fi)] fifth generation (5G) architecture for autonomous vehicular communication applications. The hybrid multiple input multiple output (MIMO) system architecture design is mathematically modelled and presented. The reported prelim PoC validation focuses on the Li-Fi experiment and results. The proposed hybrid system's effectiveness was evaluated using the open-source "Model-based Autonomous Traffic Simulation" (MOBATSim). The simulation results of a potential Li-Fi system and a PoC prototype are presented to demonstrate the role of the Li-Fi system in the proposed hybrid mmWave-Li-Fi 5G architecture. Three models of LED/lamp and two models of photodiode were simulated at three different vehicle speeds to ascertain the potential of the system. Promising results are reported at low speeds with received power values of up to -8.39 dBm and signal-to-noise ratios of up to 29.39 dB. Practical prototype simulations showed auspicious results including received power of -24.6 dBm to -34.12 dBm at the vehicle speeds of 10 MPH to 30 MPH respectively. The implemented PoC Li-Fi technology component has demonstrated the ability to transmit information with a theoretical output of 333 bits per second at 1.92 m, without the use of any high-power processors, components, and modulation techniques. The proposed system yields high data rates due to reconfigurable high bandwidth channels; many simultaneous multimedia mmWave-Li-Fi connections enabled due to spatial reuse with narrow beams; and easier mmWave-Li-Fi ultra-low latency support occasioned by smaller packet sizes. This holds a great promise for the hybrid 5G/6G mmWave-Li-Fi autonomous vehicular communication use case and/or applications.

INDEX TERMS 6G, 5G mmWave-Li-Fi communication, autonomous vehicle, holographic, free-space optics, hybrid MIMO beamforming, reconfigurable.

I. INTRODUCTION

Autonomously operating vehicles have been extensively researched and developed effective 2000 [1], [2], [3]. This has been propelled by the major advances in the active

semiconductor devices, processor, and artificial intelligence technologies in the past decade [3], [4]. Modern vehicles incorporate many advanced driver assistance systems (ADAS) which utilise sensors such as ultrasonic, radio detection and ranging (RADAR), light detection and ranging (LIDAR), and image recognition from camera feeds. These devices process ever increasing amounts of data to

The associate editor coordinating the review of this manuscript and approving it for publication was Bilal Khawaja^{ID}.

be able to achieve the required levels of safe autonomous driving. They utilize a superfluous approach that relies on large software updates for complex mapping data delivered over congested fourth-generation (4G) and 5G networks. Despite the increase in the capabilities of the autonomous functions of vehicles in the last decade, it is more apparent than ever that a more connected approach – in which data are shared effectively between vehicles and/or infrastructure – is needed. By conglomerating raw compute performance and the massive amounts of information available among individual vehicles and infrastructure, a true capability-based autonomous operation of vehicles will be achieved [5], [6], [7], [8], [9], [10].

Communication standards [11], [12], [13], [14] have been set out by organisations worldwide, such as the Third Generation Partnership Project (3GPP) to harmonise vehicle-to-vehicle (V2V); vehicle-to-infrastructure (V2I); and vehicle-to-everything (V2X) communications standards. They utilise cutting-edge technologies including mmWave 5G New Radio (NR) to provide gigabit speeds at ultra-low latency. IEEE 802.11p is based on Wi-Fi and is the sole standardised implementation to be utilized in a commercial vehicle [15], [16], [17], [18], [19], [20].

This paper aims to demonstrate how current standards could be adapted to create a more robust co-operative hybrid architecture, utilizing both mmWave 5G and Li-Fi [14], [15], [16], [17], [18]. Current standards rely on technologies that are hindered by limited range, which can be increased at the cost of speed and latency in a typical conventional approach. A low-cost, easy-to-implement solution to this is a Li-Fi system that offers high speed, and low-latency connectivity utilising the visible light spectrum. A Li-Fi-only solution relies heavily on a line-of-sight (LoS) signal propagation and high-powered light emitting sources and/or high sensitivity photodiodes for a reliable transmission. However, it has a promising potential as a stop-gap solution for sub-optimal conditions for RF-based technologies. Hence, a hybrid multiple input multiple output (MIMO) beamformed mmWave-Li-Fi 5G communication is a holy grail for autonomous vehicular communication use case and/or applications [4], [5], [6], [7], [8], [9].

The novelty of the proposed mmWave-Li-Fi system revolves around (i) hybrid multimedia high data rates due to reconfigurable high bandwidth channels; (ii) many simultaneous multimedia mmWave-Li-Fi connections enabled due to spatial reuse with narrow beams; (iii) easier mmWave-Li-Fi ultra-low latency support occasioned by smaller packet sizes; and (iv) three operational adaptive beamforming modes for variable multimedia data rate and latency spanning short- and long-range 5G/6G vehicular communication use cases/applications.

II. EMERGING VEHICULAR COMMUNICATION USE CASES AND APPLICATIONS

The multidimensional objectives of mmWave 5G radio access technology (RAT) span higher data rates to lower latency, viz:

peak data rate, area traffic capacity, user experience data rate, spectrum efficiency, energy efficiency, connection density, latency, and mobility.

The emerging industry verticals for hybrid mmWave-FSO 5G communication include thus: autonomous automotive; critical telemedicine/e-health; energy; media and entertainment; smart manufacturing/factory of the future. The autonomous automotive industry is leading the way in key requirements for the development of hybrid mmWave-FSO 5G use cases and/or applications.

The leading mmWave autonomous automotive use case and/or application domains span thus:

- Vehicle-to-infrastructure (V2X) for traffic efficiency (requirement: low latency but low-rate connectivity may be sufficient)
- V2X for advanced driver assistance systems (requirement: low latency but modest data rate requirements for alerting driver; High data rate if “see through” capability is included)
- V2X for fully automated driving (requirement: full automation requires Gbps data rates and millisecond (ms) latencies)
- V2X for traffic efficiency (requirement: low latency but low-rate connectivity may be sufficient).

III. HYBRID MILLIMETRE-WAVE-FSO 5G MIMO BEAMFORMER ARCHITECTURE AND MODEL

A. HYBRID mmWave-FSO SYSTEM ARCHITECTURE

A hybrid adaptive MIMO technique that continuously, dynamically, seamlessly, and ubiquitously update their real-time parametric data from the received (input) signals (Fig. 1) [5] is proposed in this paper. The generic mmWave-FSO architecture of a hybrid broadband communication system comprises an array of multi-radio standards sensors in tandem with multimedia tapped-delay lines and finite impulse response filter networks [5], [6], [7].

The hybrid mmWave-Li-Fi MIMO beamformer enables reliable, power-efficient, low-cost, and scalable over-the-air multi-radio access technology solutions implementations. The regulated-element hybrid mmWave-Li-Fi MIMO beamformer delivers low-component, and low-carbon footprints; scalable; reliable; and high-gain multi-radio beamformer architecture [5]. The proposed mmWave-Li-Fi beamformer array of sensors contains a network of transversal finite impulse response (FIR) filters, tapped-delay lines, and an adjustable element-dependent feedback system [5]. The deterministic use case and/or application data rate and latency requirements determine the choice of the radio communication medium technology. Depending on the chosen radio transmission and reception technology (mmWave or Li-Fi), the noise condition of each sensor node, and the channel state, the received input and the signal filter outputs, selectively yield the feedback outputs [5], [6], [7]. The REF beamformer architecture (Fig. 1) contains a mmWave-Li-Fi MIMO bus system for selectively adapting the dynamic system radio communication technology and noise to the optimal

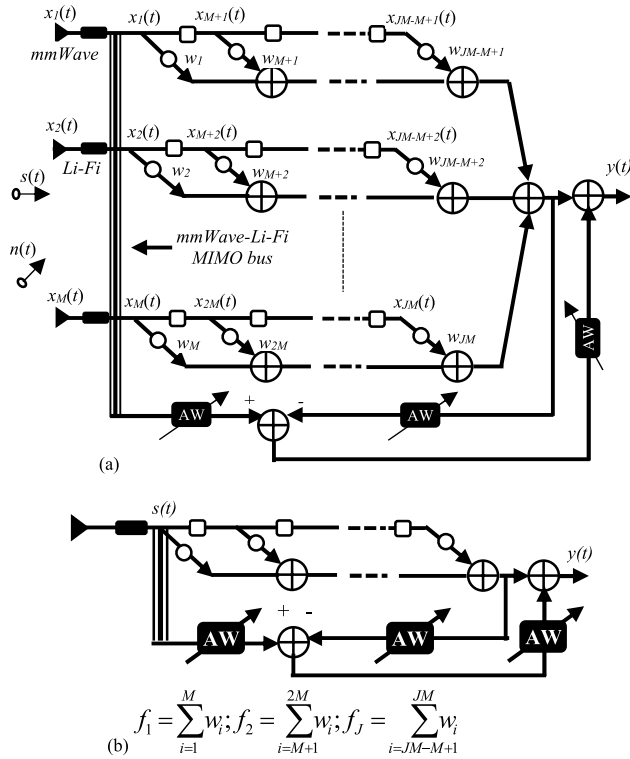


FIGURE 1. Hybrid mmWave-Li-Fi MIMO system model architecture (a) Expanded version (b) Condensed version [5].

performance requirement of the overall hybrid linear array. The REF architecture deterministically tracks the mmWave channel noise source behaviour, activating the mmWave-to-Li-Fi handover based on a variable threshold V2X data rate (Gbps) and latency margin (ms).

B. HYBRID mmWave-Li-Fi SYSTEM MODEL ANALYSIS

The mmWave-Li-Fi adaptive beamforming method is a constrained optimization function of the form defined by:

$$\text{minimize } \mathbf{w}^T \mathbf{R}_{hxx} \mathbf{w} \quad (1)$$

$$\text{subject to } \mathbf{C}_h^T \mathbf{w} = \mathbf{f}_h \quad (2)$$

where \mathbf{C}_h is the hybrid multimedia constraint matrix, \mathbf{f}_h , the constrained hybrid system impulse response, and \mathbf{R}_{hxx} , the hybrid multimedia autocorrelation matrix. The sum of the FIR filter outputs gives the output of the hybrid mmWave-Li-Fi beamformer, $y_h(t) = \mathbf{w}^T \mathbf{x}_h(t)$. The optimum weight vector, \mathbf{w}_{opt} , is obtained as follows: [5]

$$\mathbf{w}_{\text{hopt}} = \mathbf{R}_{hxx}^{-1} \mathbf{C}_h \left(\mathbf{C}_h^T \mathbf{R}_{hxx}^{-1} \mathbf{C}_h \right)^{-1} \mathbf{f}_h \quad (3)$$

where the initial weight vector, $\mathbf{w}_h[0] = \mathbf{f}$. The corresponding system impulse response vector, \mathbf{f}_{hir} , is given by [5]:

$$\mathbf{f}_{\text{hir}} = \mathbf{C}_h \left(\mathbf{C}_h^T \mathbf{C}_h \right)^{-1} \mathbf{f} \quad (4)$$

The presented Regulated-Element Multimedia (REM) mmWave-Li-Fi beamforming algorithm chooses weights to

minimize the mean square error between the beamformer output and the reference signal using an adaptive detection of the received signal at each multi-media sensor. The regulated feedback system of the REM beamformer enables an optimal noise reduction. The required FIR filter taps are 50% lower than the conventional Frost method for a 6-dB mmWave-Li-Fi array gain increase capability [5]. The matrix form of the constraint functions of the REM beamformer is given by:

$$\mathbf{W} \begin{bmatrix} 1 \\ 1 \\ \vdots \\ 1 \end{bmatrix} = \begin{bmatrix} f_1 \\ f_2 \\ \vdots \\ f_J \end{bmatrix} \quad (5)$$

where the weight matrix, \mathbf{W} , is given by:

$$\mathbf{W} = \begin{bmatrix} \mathbf{w}_1 & \mathbf{w}_2 & \cdot & \cdot & \cdot & \mathbf{w}_M \\ \mathbf{w}_{M+1} & \mathbf{w}_{M+2} & \cdot & \cdot & \cdot & \mathbf{w}_{2M} \\ \vdots & \vdots & & & & \vdots \\ \mathbf{w}_{JM-M+1} & \mathbf{w}_{JM-M+2} & & & & \mathbf{w}_{JM} \end{bmatrix} \quad (6)$$

and the hybrid mmWave-Li-Fi system impulse response, \mathbf{f}_h , is obtained as a J -dimensional vector thus [5]:

$$\mathbf{f}_h = [f_1, f_2, \dots, f_J]^T \quad (7)$$

where $f_1 = \sum_{i=1}^M w_i$, $f_2 = \sum_{i=M+1}^{2M} w_i$, $f_J = \sum_{i=JM-M+1}^{JM} w_i$.

The noisy signals, $x_h(n)$, and the weight vector, \mathbf{w}_h , can be derived for alternative odd and even integrated hybrid mmWave-Li-Fi taps. The constrained hybrid mmWave-Li-Fi system impulse response, \mathbf{f}_h , and the matrix of JM column vectors, \mathbf{C}_h , are utilized for the multimedia constraint formulation. These parameters are obtained as follows:

$$\begin{aligned} \mathbf{x}_h^T(n) &= [x_1(n) \quad x_2(n) \quad \cdot \quad \cdot \quad \cdot \quad x_{JM}(n)], \\ \mathbf{w}_h^T &= [w_1 \quad w_2 \quad \cdot \quad \cdot \quad \cdot \quad w_{JM}], \\ \mathbf{f}_{\text{hir}}^T &= [f_1 \quad f_2 \quad \cdot \quad \cdot \quad \cdot \quad f_{JM}], \\ \mathbf{C}_h &= [c_1, \quad c_2, \quad \cdot \quad \cdot \quad \cdot, \quad c_J]. \end{aligned}$$

For J FIR filter coefficients and M sensors, the entries, c_i , of the constraint matrix, \mathbf{C} , are the column vectors of length JM with $(i-1)M$ zeros followed by M ones and $(J-i)M$ zeros. For a 4-element uniform linear mmWave-Li-Fi array system deploying 4 FIR filter taps. The constraint matrix, \mathbf{C} , is given by:

$$\mathbf{C} = [c_1, c_2, c_3, c_4]$$

where the entries c_i [$i = 1$ to 4 (the number of filter taps)] are obtained as c_1 – c_4 , shown at the bottom of the next page.

The expected mmWave-Li-Fi beamformer array output can be formulated for three use cases, viz:

Case 1: mmWave signals are transmitted and received on all the activated sensors.

Case 2: mmWave and Li-Fi, the deterministic data transmission distribution is a function of the data rate and the latency requirements of the application. mmWave and Li-Fi signals are complementarily transmitted and received respecting the defined system performance metrics (such as variable data rate and variable latency)

Case 3: Li-Fi signals are transmitted and received on all the activated sensors.

The received signal vector, $S(t)$, for the entire uniform linear mmWave-Li-Fi array (Fig. 1) is given by:

$$S_r(t) = \sum_{i=1}^M x_i(t) \quad (8)$$

where the received signal at each sensor, $x_i(t)$, is given as a function of the received desired signal, $s_i(t)$, and dynamic system noise, $n_i(t)$, thus:

$$x_i(t) = s_i(t) + n_i(t) \quad (9)$$

The multimedia residual noise, n'_o , is obtained as a function of the expected (mean average) output signal of the hybrid MIMO mmWave-Li-Fi array, $E[y^2(n)]$, the received signal at the time of n th sample, $S_r(n)$, and the number of sensors, M , thus: [5]

$$n'_o(n) = \frac{S_r(n)}{M} - ME[y^2(n)] \quad (10)$$

Mathematically, the REM beamformer array output gain, $REM_o(n)$, is obtained (with recourse to Fig. 1) from (1), and (8) to (10) as: [5]

$$REM_o(n) = \frac{1}{M^{2M}} \times \left(M^{M+1} (M^{M-1} - 1) w^T R_{xx} w + \sum_{i=1}^M x_i(n) \right) \quad (11)$$

Whilst (12) yields a high multimedia array gain for an appreciable residual noise reduction, the cumulative variable array signal gain reduces by M^{-2M} as the number of multimedia sensors increases beyond a threshold number. This occasions an array compression phenomenon with an increasing number of enabled active elements beyond the threshold number. This challenge is overcome by deriving a hybrid REM beamformer with the individual array elements enabled for a M^{-2} feedback threshold factor at the time of the received n th sample, $S_r(n)$ [5]. The residual noise [5] of the hybrid REM beamformer, n'_r , is estimated with recourse to Fig. 1 and (8) to (10).

The overall output of the hybrid REM beamformer is obtained by enabling multimedia array element-dependent Adjustable Weight (AW) vectors. Hence, the hybrid REM beamformer output, $REM_h(n)$, is given by:

$$REM_h(n) = \frac{1}{M^2} \left(M(M-1) E[y^2(n)] + \sum_{i=1}^M (x_{ri}(n)) \right) \quad (12)$$

For the example 4-sensor mmWave-Li-Fi system with 4 FIR taps, we assume that odd- and even-numbered MIMO sensors are mmWave and Li-Fi respectively. A summary of the weight vectors, w , for a three-mode operation can be obtained thus:

(i) **Mode 1: mmWave Data Transmission and Reception Only**

$$W = \begin{bmatrix} w_1 & w_3 & \cdot & \cdot & \cdot & w_{M-1} \\ w_{M+1} & w_{M+3} & \cdot & \cdot & \cdot & w_{2M-1} \\ \cdot & \cdot & & & & \\ \cdot & \cdot & & & & \\ \cdot & \cdot & & & & \\ w_{JM-M+1} & w_{JM-M+3} & & & & w_{JM-1} \end{bmatrix} \quad (13)$$

The corresponding impulse response, f_{mmWave} , is thus:

$$f_{mmWave} = \begin{bmatrix} W_1 & + & W_3 \\ W_5 & + & W_7 \\ \cdot & + & \cdot \\ \cdot & + & \cdot \\ W_{13} & + & W_{15} \end{bmatrix}$$

(ii) **Mode 2: Li-Fi Data Transmission and Reception Only**

$$W = \begin{bmatrix} w_2 & w_4 & \cdot & \cdot & \cdot & w_M \\ w_{M+2} & w_{M+4} & \cdot & \cdot & \cdot & w_{2M} \\ \cdot & \cdot & & & & \\ \cdot & \cdot & & & & \\ \cdot & \cdot & & & & \\ w_{JM-M+2} & w_{JM-M+4} & & & & w_{JM} \end{bmatrix} \quad (14)$$

The corresponding impulse response, f_{Li-Fi} , is thus:

$$f_{Li-Fi} = \begin{bmatrix} W_2 & + & W_4 \\ W_6 & + & W_8 \\ \cdot & + & \cdot \\ \cdot & + & \cdot \\ W_{14} & + & W_{16} \end{bmatrix}$$

$$\begin{aligned} c_1 &= [1 \ 1 \ 1 \ 1 \ 0 \ 0 \ 0 \ 0 \ 0 \ 0 \ 0 \ 0 \ 0 \ 0 \ 0 \ 0] \\ c_2 &= [0 \ 0 \ 0 \ 0 \ 1 \ 1 \ 1 \ 1 \ 0 \ 0 \ 0 \ 0 \ 0 \ 0 \ 0 \ 0] \\ c_3 &= [0 \ 0 \ 0 \ 0 \ 0 \ 0 \ 0 \ 0 \ 1 \ 1 \ 1 \ 1 \ 0 \ 0 \ 0 \ 0] \\ c_4 &= [0 \ 0 \ 0 \ 0 \ 0 \ 0 \ 0 \ 0 \ 0 \ 0 \ 0 \ 0 \ 1 \ 1 \ 1 \ 1] \end{aligned}$$

(iii) **Mode 3: Simultaneous Hybrid mmWave-Li-Fi Connectivity**

$$W = \begin{bmatrix} w_1 & w_2 & \cdot & \cdot & \cdot & w_M \\ w_{M+1} & w_{M+2} & \cdot & \cdot & \cdot & w_{2M} \\ \cdot & \cdot & \cdot & \cdot & \cdot & \cdot \\ \cdot & \cdot & \cdot & \cdot & \cdot & \cdot \\ w_{JM-M+1} & w_{JM-M+2} & \cdot & \cdot & \cdot & w_{JM} \end{bmatrix} \quad (15)$$

The corresponding hybrid multimedia impulse response, f_h , is thus:

$$f_1 = \sum_{i=1}^M w_i; \quad f_2 = \sum_{i=M+1}^{2M} w_i; \quad f_J = \sum_{i=JM-M+1}^{JM} w_i$$

IV. SYSTEM METHODOLOGY AND SIMULATION

This section explores the potential performance and feasibility of the Li-Fi system in the proposed hybrid mmWave-Li-Fi connectivity architecture. The presented Li-Fi system simulation is based on the indoor optical wireless line-of-sight (LoS) propagation model [5]. This model calculated the power received and signal-to-noise ratio (SNR) to compare the different light emitting sources. The model is ideal and assumes no attenuation effects due to environmental and atmospheric conditions.

$$P_{Received} = P_{TX} \times H \quad (16)$$

where $P_{Received}$ = Power Received in Watt; P_{TX} = Output power of the LED in Watts; and H = DC Channel Gain and given by:

$$H = \frac{A(m+1)}{2\pi d^2} \cos^m(\phi) T_s(\Psi) g(\Psi) \cos(\Psi) \quad (17)$$

where A = Active Photodiode Area (m^2); m = Lambert's Mode; d = Diameter of the Photodiode (m); ϕ = Semi-angle at Half Power-irradiance (deg); and Ψ = Incident Angle to the Photodetector (deg).

$$SNR = \frac{(R^2 \times (P \times 10^{-6})^2)}{\text{Bit Rate} \times \text{Noise Spectral Density}} \quad (18)$$

where R = Photodiode Responsivity (AW^{-1}); and P = Power Received in Watt.

Two models (Table 1) of photodiode were simulated at a range of vehicle speeds to determine the overall performance of the light emission sources being tested (Table 2) for a MIMO Li-Fi implementation consideration.

To calculate the distance between the transmitters and receivers at a given vehicle speed in the simulation, it is assumed that the 2-second gap rule is followed as set out by UK guidelines on road safety [36].

A Proof-of-Concept (PoC) prototype was created to analyse the practical range of the system and to demonstrate the feasibility of the role of Li-Fi in the hybrid system. This prototype was tested with three types of light emitting sources (Table 3 & Figs. 2 and 3).

TABLE 1. Photodiode parameters for Li-Fi system simulation.

Parameter	HAMAMATSU S9648-200SB 'Practical Photodiode'	OSI OPTOELECTRONICS PIN-25D 'Ideal Photodiode'
Active Area	$1.472e^{-5} m^2$	$6.130e^{-4} m^2$
FOV	63.00°	56.85°
Sensitivity	0.53	0.65
Refractive Index	1.5	1.0

TABLE 2. Light emitting source parameters for Li-Fi system simulation.

Parameter	NICHIA NSDW570GS- K1	QASIM QA- TL0210-7443- W	YOLVINUO H7
Operating Voltage	3.7V	12V	12V
Transmit Power	0.296W	5.16W	36W
Bulb Technology	LED	LED	LED

TABLE 3. Light emitting source parameters for proof-of-concept prototype.

Parameter	NICHIA NSDW570GS- K1	QASIM QA- TL0210-7443-W	BOSCH 1987301079
Operating Voltage	3.7V	12V	12V
Transmit Power	0.296W	5.160W	5.00W
Bulb Technology	LED	LED	HALOGEN
Package Type	Through-Hole	7443 W21	7443 W21

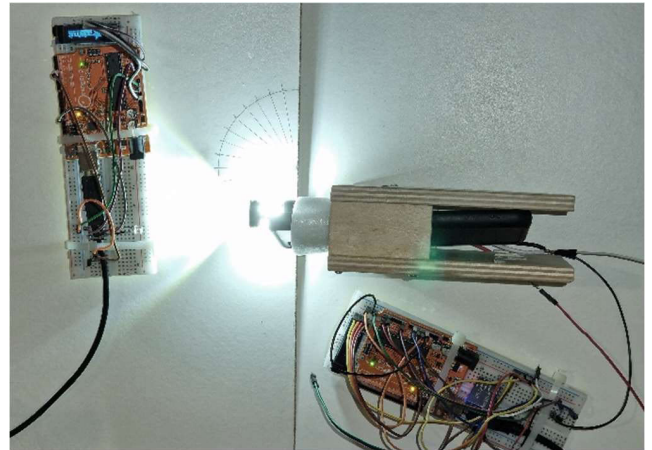


FIGURE 2. PoC prototype testing QASIM QA-TL0210-7443-W.

The PoC system consists of one transmitter and one receiver as the bare minimum to demonstrate the system's capability. Both units utilise the Arduino Uno which is a development board based on the ATMEGA328P microcontroller. Although the overall hybrid architecture will have to utilise a much higher power processor, the Arduino Uno was chosen solely on cost and ease of development. The transmitter unit utilises a HC-05 Bluetooth module to establish a connection with a Bluetooth On-Board

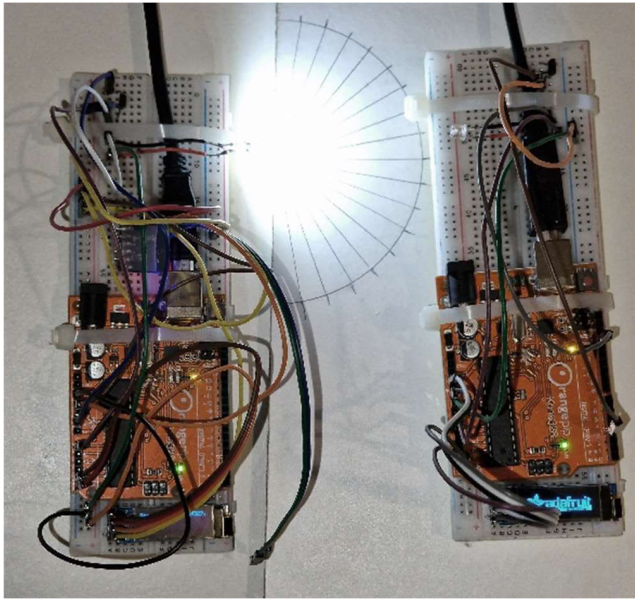


FIGURE 3. PoC prototype testing NICHIA NSDW570GS-K1.

Diagnostics II (OBDII) reader to retrieve and interpret data from a live controller area network (CAN) bus system in a vehicle. CAN bus is a serial communication message broadcast system that interfaces several systems and micro-controllers together to create a cohesive and reliable serial communication system for microcontrollers found in modern vehicles responsible for the fundamental operation of the vehicles systems. Rather than sending specific messages between nodes on the network, the CAN bus system relies on broadcasting messages to all nodes at a maximum rate of 1 Mbps according to the ISO-11898 standard [37].

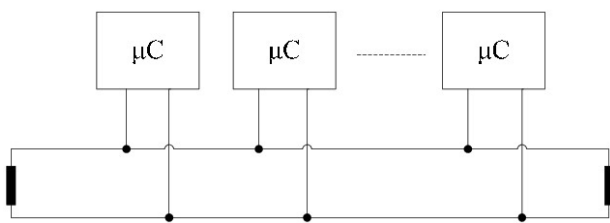


FIGURE 4. Generic CAN bus topology [37].

The CAN bus standard includes specifications for OBDII which is a defined standard for retrieving diagnostic information from vehicles. These data include, but are not limited to, vehicle speed, engine revolutions per minute (RPM), and throttle position. These are values which can be used to determine whether the vehicle is in motion and whether it is accelerating but cannot be used to deduce current or predicted vehicle motion and positioning, as this data is not considered diagnostic data and is therefore obfuscated behind manufacturer specific implementations of various systems.

I2C displays are utilised to display the data being transmitted and received on each unit respectively. The open-source

library “ELMDuino” [21] is used to send the correct CAN messages to retrieve specific diagnostic data from the OBDII port on the transmitter. The data retrieved via the OBDII port is saved as a string, before being converted into an 8-bit binary value and transmitted via a software-defined serial bus to the light emitting source. This data is received as an analogue light reading from the photodiode in the receiver and compared with a threshold light level to determine whether the received bit is a “1” or “0.” The received binary string is then converted into a float value and displayed. The analogue threshold light level can be converted into lux by converting the analogue reading into voltage; the photocurrent can be deduced and compared with the photocurrent-illuminance profile for the photodiode (provided in the manufacturer’s datasheet). The length of the binary string is assumed on the receiver with a short delay in between transmission strings to denote the end of transmission periods.

V. EXPERIMENTAL CONSIDERATIONS AND ANALYSIS

A. CONSIDERATIONS FOR THE SIMULATION OF THE Li-Fi SYSTEM

The major control variable is the light emitting source used in the simulations and the parameters are based on commercial products. Two models of photodiode were also simulated (Figs. 6 and 7). The “practical photodiode” is the component utilized in the PoC; and the “ideal photodiode” is a commercially available component with ideal parameters. The distance between the transmitters and the receivers is determined at a range of vehicle speeds. This is utilized to create a profile of the simulated components. The components chosen for the simulation are used mainly to demonstrate the relationships between the output power, and the distance. The target signal level is at 15 dBm (minimum, suitable for Mode 2 operation) and 25 dBm (suitable for Mode 3 operation) for a reliable signal. For a variable mmWave-Li-Fi 5G transceiver, the active semiconductor devices process technologies and subsystem design topology determine the receiver sensitivity [22], [23], [24], [25], [26], [27], [28].

B. CONSIDERATIONS FOR THE PROOF-OF-CONCEPT PROTOTYPE Li-Fi SYSTEM

The PoC system was constructed and tested using different LED-based Li-Fi systems at different vehicle speeds. The major control variable in the testing of the PoC is the light emitting source. The results for each light emitting source were tested thrice and averaged to produce the final performance metrics. A halogen bulb was utilized solely to demonstrate the importance of using the LED technology for the Li-Fi communication. The YOLVINUO H7 prototype performance metrics are significantly influenced by the power supply output limitation. Moreover, the ideal photodiode could not be obtained for testing due to budget constraints. The results recorded were achieved within a 1-hour time frame on the day of testing to ensure minimum variance in background light and weather conditions. The transmitter was connected

to a live CAN Bus system via a Bluetooth OBDII Reader plugged into the OBDII port, standard on most vehicles post 1996 [37]. The Bluetooth OBDII reader was paired with the HC-05 modules connected to the hardware serial port on the transmitter. The distance between the transmitter and receiver was then gradually increased in 10 mm increments until the receiver could no longer interpret the sent data from the transmitter.

VI. RESULTS AND DISCUSSION

A. RESULTS OF SIMULATED Li-Fi SYSTEM

The practical photodiode (Figs. 4 and 5) must overcome the poor SNR for an appreciable V2X data communication link performance [29], [30], [31]. Considering the best-case scenario, the 36-W YOLVINUO H7 with the vehicle travelling at 10 MPH, the received power at the receiver is not in a range that can be deemed suitable for V2V communication. This means that when it comes to the commercial implementation of the hybrid system, the implemented and presented photodiode will require an increase in sensitivity and active surface area [30], [31]. Otherwise, the system will only be suitable for short-range communications when the vehicles are close to each other or stationary; this places a higher reliance on Mode 1 and Mode 3 modes of operation, diminishing the intended use case of the hybrid system. Thus, a higher power light emission source should be considered to maximize the distance the signal can be transmitted, without

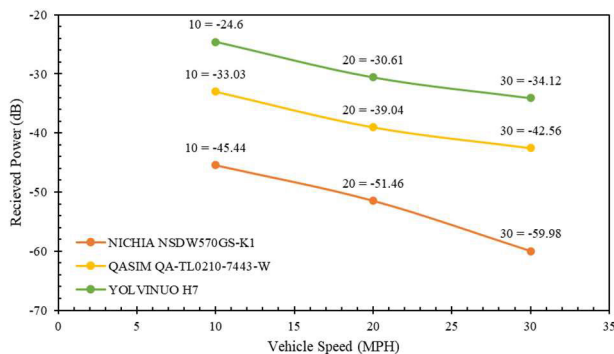


FIGURE 5. Received power for practical photodiode.

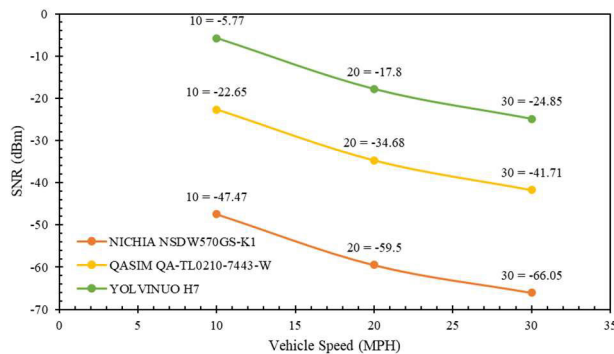


FIGURE 6. Signal to noise ratio for a practical photodiode.

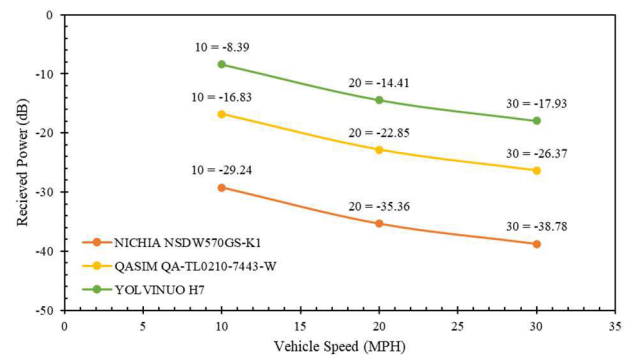


FIGURE 7. Received power for an ideal photodiode.

reliance on Mode 1 and 2 in the hybrid architecture. However, the ideal photodiode can receive the same power levels of the simulated test signal at a better suited power and SNR value. The results reveal that only the YOLVINUO H7 can maintain a feasible SNR response. This means that, in theory, the proposed hybrid system could feasibly employ the use of Modes 2 and 3 operations to allow for more robust and reliable communication. In practice, the Li-Fi component still lacks favourable transmission speeds to be considered practical in these modes.

B. RESULTS OF THE PROOF-OF-CONCEPT Li-Fi SYSTEM

The PoC results (Figs. 9 and 10) successfully demonstrate the relationship between power and distance, and that increasing the output power of the transmitter results in longer transmission distances without data loss (within the limitations of the practical prototype). However, both the NICHIA NSDW570GS-K1 and the QASIM QA-TL0210-7443-W bulbs are limited to a maximum transfer rate of 2 bits per second (bps). This is well below the targeted data rate of 1 Mbps due to the limitations of the development board. The observed bitrates from the preliminary testing and PoC indicate that the bottleneck in transmission speed is caused by the lack of processing power. Theoretically, as the distance decreases, the maximum achievable data rate should have been closer to at least the results achieved in the preliminary

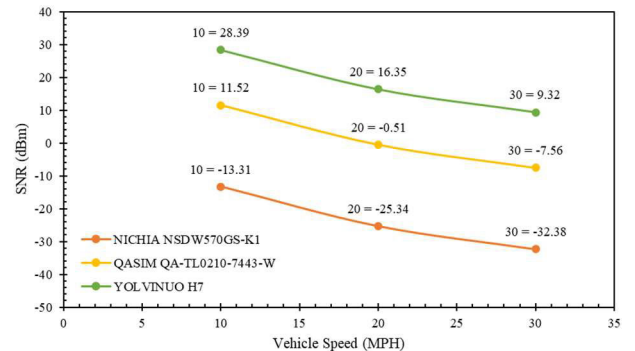


FIGURE 8. Signal to noise ratio for an ideal photodiode.

TABLE 4. Comparison of results with the previous studies.

SOURCE	VLC MAXIMUM DATA RATE	LATENCY MODE	OPERATIONAL BEAMFORMING MODES	TRANSMISSION DISTANCE	MODULATION TECHNIQUES	USE CASE
[32]	Up to 1.84 Gbps	Fixed	2 (mmWave and Li-Fi)	1.1 m	Direct Current biased Optical Orthogonal Frequency Division Multiplexing Intensity Modulation	General-purpose Hybrid mmWave-VLC System
[33]	15.73 Gbps	Fixed	1 (Li-Fi)	1.6 m	Direct Detection Direct Current-biased Optical Orthogonal Frequency Division Multiplexing	VLC Communication System
[34]	Up to 200 Mbps	Fixed	2 (mmWave and Li-Fi)	45 m	Direct Current-biased Optical Orthogonal Frequency Division Multiplexing	Indoor hybrid mmWave Wi-Fi 6 / Li-Fi Access Point
[35]	Up to approx. 270 Mbps	Fixed	1 (Li-Fi)	14 m	Time Division Multiple Access	Indoor parallel Transmission Li-Fi Communications System
This work	Dynamic / Variable (2 bps – Gbps)	Dynamic (Reconfigurable / Variable)	3 (mmWave, Li-Fi, and Simultaneous mmWave-Li-Fi / Adaptive MIMO Beamforming)	17.8+ m (for an acceptable SNR)	Direct Detection	Hybrid/Multimedia mmWave-Li-Fi communication system for V2X Applications

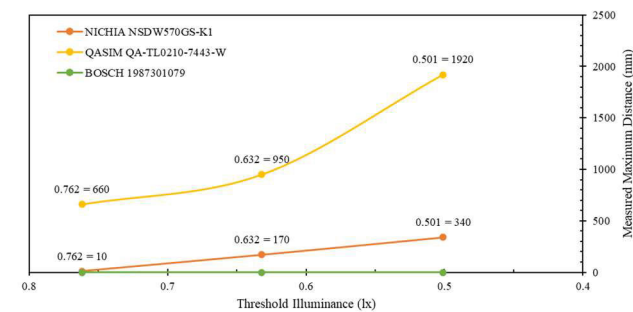


FIGURE 9. Measured maximum distance at different illuminance threshold levels. (No data labels shown for BOSCH 1987301079, all values are 0).

testing. However, this was not the case – the preliminary testing also yielded the same response.

C. PATH FOR FURTHER DEVELOPMENT OF PROOF-OF-CONCEPT Li-Fi SYSTEM FOR FULL INTEGRATION INTO A HYBRID mmWave-Li-Fi ARCHITECTURE

The results from the simulation and PoC system (Fig. 9) demonstrate that the current implementation is unfeasible in its current state and that a more robust PoC must be made to demonstrate more favourable and realistic results before

further practical implementation. The main limitation of the PoC was the Arduino Uno (in the transmitter unit) with only a single serial port available. This was utilized to communicate with the vehicle CAN bus via the Bluetooth OBDII reader at the maximum achievable bitrate via the HC-05 Bluetooth module. As the hardware serial port was occupied, the Li-Fi signal was transmitted over software serial through the digital output pins. Thus, a limitation by the clock speed and processing power of the microcontroller was encountered, hindering maximum achievable bitrate during the transmission. In the receiver, the same limitations with clock speed and processing power were observed - though to a lesser degree than demonstrated on the transmitter. The receiver unit had less performance overheads compared with the transmitter (which enabled the maximum downlink rate of 333 bits achieved in the prelim testing). These limitations prevented the receiver unit from achieving the targeted real-time bitrate of 1 Mbps. Moreover, utilizing a development board with a minimum of three hardware serial ports [for a minimum single input single output (SISO)], and a more powerful processor would boost the data rate of the Li-Fi system. For our future PoC system design, a higher power development board and/or a field programmable gate array (FPGA) development kit will be more suitable for the application. This would allow for

a low-latency and deterministic hardware-in-the-loop implementation and validation of the proposed hybrid architecture. The FPGA would potentially provide more efficient processing power capability. This would also enable the use of a MIMO architecture type to achieve increased performance metrics by utilising multiple RF/mmWave nodes for non-LOS communication. Moreover, an advanced powerful processor or FPGA would allow for advanced modulation schemes (such as quadrature amplitude modulation) to be deployed. The implementation of techniques including clock synchronization and error correction algorithms would further improve the reliability of transmission by reducing the bit error rate. Deploying reconfigurable MIMO antenna frontend subsystems would increase the data throughput [19]. An industry-grade commercial implementation of the proposed hybrid mmWave-Li-Fi system requires a direct link to the vehicles' CAN bus system with a manufacturer-specific integration. This would allow access and control of a larger range of data and systems than just the standard diagnostic data. Thus, enabling higher levels of autonomous operation for vehicles. It has been demonstrated in the simulations of the Li-Fi system that using the LED technology demonstrated in the simulations and PoC is unfeasible. A purpose-made unit would have to be designed, potentially employing the use of light amplification by stimulated emission of radiation (LASER) technology or high-power LEDs. This will still adhere to the current legislation(s) governing headlights on vehicles to ensure the safety of other road users. The potential use of alternative active semiconductor devices process technologies for the photodetector is worthy of consideration.

In the proposed hybrid architecture, fuzzification and defuzzification can play a role in switching logic for the proposed operating modes. By being able to substantiate multiple variables from the respective transmitters and receivers, the optimal operating modes can be selected on combination of multiple variables rather than just comparing single values. By comparing values from the transceivers to the 5G performance metrics for ultra-reliable and low-latency communication (URLLC), the most optimum mode of transmission can be deduced even when the conditions or values for any given mode of transmission are not optimal. In this paper, a low-latency deterministic switching mode is adopted using the parallel IP logic blocks of the FPGA. The signal reaching the hybrid MIMO mmWave-Li-Fi system is received and processed within its relevant transceiver chain. Hence, both bipolar complex signals and unipolar real-valued waveforms are accommodated.

The sufficient proof-of-concept demonstration reported in this paper revolves around the three-mode mmWave-Li-Fi system architecture design and the mathematical model development. The authors have included a simulated validated truth table (Table 5) for the role of switching between the modes using a FPGA. FPGA devices support both functional and timing simulations. For n number of MIMO mmWave and Li-Fi inputs, there is a corresponding 2^n number of test vectors to be generated and used for the system

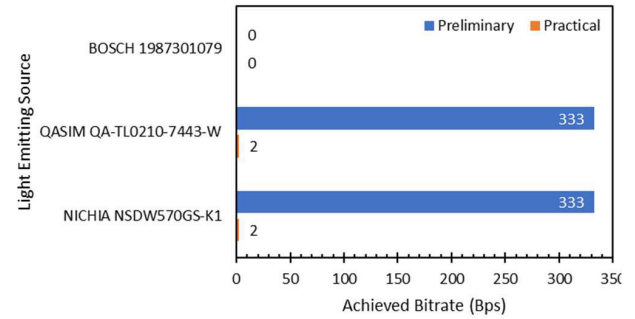


FIGURE 10. Preliminary and PoC achieved bitrate.

simulation. This was implemented to accommodate the functional and timing simulations of two identical MIMO transceivers. The reported designed digital circuits were simulated using the Quartus II Simulator.

In a functional simulation, it is assumed that the logic blocks/elements and interconnects within the FPGA fabric are perfect with no signal propagation delays. It is mostly used to ascertain the functional integrity of a circuit at the design stage. It has a low latency since the simulation uses the logic expressions that characterise the digital circuit. The timing simulation takes the signal propagation through the circuit into consideration; it tests the fitter circuit to authenticate its functional correctness and timing.

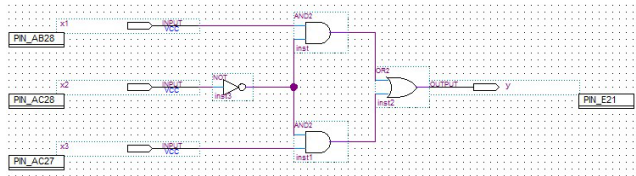
The logic sequence is described below:

- output: $y = 1$ (Transmit/Receive Data; Transmitter (Tx) / Receiver (Rx) On for mmWave / Li-Fi; [Data Rate, Latency] = [Low / High, Low / High]);
- inputs:
 - $x_3 = 1$ (Data Transmission Request Detected or favourable channel conditions);
 - $x_1 = 1$ (Transmit data using mmWave 5G);
 - $x_2 = 0$ (Tx/Rx Shutdown).
- The mmWave MIMO Transceiver should transmit data when unfavourable channel conditions are detected for Li-Fi (low-to-high data rate and low-to-medium latency; $x_1 = 1$; $x_2 = 0$; $x_3 = 0$)
- The Li-Fi MIMO Transceiver should transmit data when favourable channel conditions are detected for Li-Fi (high data rate and low latency; $x_1 = 0$; $x_2 = 0$; $x_3 = 1$)
- The hybrid mmWave-Li-Fi MIMO transceiver should transmit data when unfavourable (using mmWave) or favourable channel (using Li-Fi) conditions are detected for Li-Fi (low-to-high data rate and low-to-medium latency; $x_1 = 1$; $x_2 = 0$; $x_3 = 1$).

The truth table (Table 5) indicates that the hybrid MIMO mmWave-Li-Fi system has a 50% probability for both mmWave and Li-Fi channels to transmit/receive data. Hence, we can enable asynchronous data transmission for variable data rate and latency requirements for autonomous vehicular communication applications. This would support meshed massive IoTs applications for long-range energy- and spectrum-efficient autonomous V2X connectivity.

TABLE 5. Truth table for the digital hybrid mmWave-Li-Fi switching modes.

X_1	X_2	X_3	Y
0	0	0	0
0	0	1	1
0	1	0	0
0	1	1	0
1	0	0	1
1	0	1	1
1	1	0	0
1	1	1	0

**FIGURE 11.** A schematic design of the three-input hybrid MIMO mmWave-Li-Fi switching modes.

Furthermore, the security of data transmission is another issue that must be investigated in our future work. Due to the nature of the data being transmitted and the role it plays in the fundamental critical systems of vehicles, it is an important point to consider. The conventional notion that Li-Fi is inherently secure due to the nature of the mode of transmission cannot be transferred to the use case(s) proposed in this paper. Because of this, the data signal must be secured by other means, such as encryption. Standards have been set out for the implementation of security features at both the physical and data link layer in visible light communication, such as ITU-TG.9991, IEEE P802.15.7 and IEEE802.11 bb [38].

D. SIMULATION FOR ANALYSIS OF EFFECTIVENESS OF HYBRID mmWave-Li-Fi ARCHITECTURE

MOBATSim is an open-source autonomous traffic simulation framework which can be used to analyse the safety of the proposed system [10]. In its default configuration, the framework assumes all vehicles have a perfect radar system and utilizes advanced cruise control systems for autonomous operation. The framework employs an ideal V2X vehicular communication system which can be adapted to simulate the hybrid system proposed. The V2X model implemented allows the individual vehicles to anticipate traffic from other vehicles and choose an optimal route. The implemented autonomous intersection management system only works for 4-way intersections. The implementation is based on different “controlled zones” where the electronic travel authorization (ETA) to respective zones is used to assign priority to vehicles entering the intersection. This could be adapted to determine an optimal priority for other junction types including T-junctions and roundabouts.

The hybrid mmWave-Li-Fi vehicular communication simulation parameters for use in the MOBATSIm are thus: vehicle position; rotation angles; vehicle size; environmental

information; vehicle speed; vehicle starting and destination points; path plans; inter-vehicular distance; city map as a diagram; front and leader vehicular distances.

VII. CONCLUSION

This paper has demonstrated that a hybrid MIMO mmWave-Li-Fi architecture could be feasible with continued development. A multimedia adaptive beamformer system architecture and a mathematical model have been presented. The practical system demonstrated utilized commercially available components and relatively less computationally intensive implementation techniques. Ultimately, the basis for a hybrid architecture has been set out and the next steps for development are clear. An increase in power is required for the light emitting source besides optimising the computational overhead. The discussed computational power required for the proposed hybrid multimedia mmWave-Li-Fi can be reduced by 50 % within the existing mm-Wave 5G communication infrastructure and/or network. For mmWave-only and Li-Fi only connectivity, the Regulated-Element Multimedia algorithm achieves variable data rate and latency with 50 % less filter weight vectors. The hybrid MIMO mmWave-Li-Fi system has a 50% probability for both mmWave and Li-Fi channels to transmit/receive data respecting the channel conditions. Besides achieving a low-carbon footprint and spectrum-efficient implementation, system reliability is boosted by deploying a dynamic hybrid mmWave-Li-Fi architecture for V2V/V2X communication ecosystem.

REFERENCES

- [1] A. Bandyopadhyay, R. Basak, I. Pal, and T. Ghosh, “Noble proposition for autonomous detection of obstacles by vehicles using the concept of light fidelity,” in *Proc. 4th Int. Conf. Electron., Mater. Eng. Nano-Technol. (IEMENTech)*, Oct. 2020, pp. 1–6, doi: [10.1109/IEMENTech51367.2020.9270054](https://doi.org/10.1109/IEMENTech51367.2020.9270054).
- [2] F. Edme, E. Bialic, and C. Chappaz, “Intelligent transportation systems & photovoltaic LiFi communication solution,” Sunpartner Technol., Rousset, France, White Paper, Feb. 2018.
- [3] K. Ganesan, P. B. Mallick, J. Lohr, D. Karampatsis, and A. Kunz, “5G V2X architecture and radio aspects,” in *Proc. IEEE Conf. Standards Commun. Neww. (CSCN)*, Oct. 2019, pp. 1–6, doi: [10.1109/CSCN.2019.8931319](https://doi.org/10.1109/CSCN.2019.8931319).
- [4] R. George, S. Vaidyanathan, A. S. Rajput, and K. Deepa (2019), “Li-Fi for vehicle-to-vehicle communication—A review,” in *Proc. Int. Conf. Recent Trends Adv. Comput.*, Jan. 2019, doi: [10.1016/j.procs.2020.01.066](https://doi.org/10.1016/j.procs.2020.01.066).
- [5] S. C. Ekpo, S. Adebisi, and A. Wells, “Regulated-element frost beam-former for vehicular multimedia sound enhancement and noise reduction applications,” *IEEE Access*, vol. 5, pp. 27254–27262, 2017, doi: [10.1109/ACCESS.2017.2775707](https://doi.org/10.1109/ACCESS.2017.2775707).
- [6] S. Enahoro, S. C. Ekpo, M. C. Uko, A. Altaf, U.-E.-H. Ansari, and M. Zafar, “Adaptive beamforming for mmWave 5G MIMO antennas,” in *Proc. IEEE 21st Annu. Wireless Microw. Technol. Conf. (WAMICON)*, Sand Key, FL, USA, Apr. 2021, pp. 1–4, doi: [10.1109/WAMICON47156.2021.9443616](https://doi.org/10.1109/WAMICON47156.2021.9443616).
- [7] S. Enahoro, S. Ekpo, and A. Gibson, “Massive multiple-input multiple-output antenna architecture for multiband 5G adaptive beamforming applications,” in *Proc. IEEE 22nd Annu. Wireless Microw. Technol. Conf. (WAMICON)*, Apr. 2022, pp. 1–4, doi: [10.1109/WAMICON53991.2022.9786100](https://doi.org/10.1109/WAMICON53991.2022.9786100).
- [8] Z. Ghassemlooy, W. Popoola, and S. Rajbhandari, *Optical Wireless Communications: System and Channel Modelling with MATLAB*, 2nd Ed. Boca Raton, FL, USA: CRC Press/Taylor & Francis Group, 2018, pp. 84–87.
- [9] S. C. Ekpo, “Parametric system engineering analysis of capability-based small satellite missions,” *IEEE Syst. J.*, vol. 13, no. 3, pp. 3546–3555, Sep. 2019, doi: [10.1109/JSYST.2019.2919526](https://doi.org/10.1109/JSYST.2019.2919526).

- [10] F. Hart, M. Saraoglu, A. Morozov, and K. Janschek, "Fail-safe priority-based approach for autonomous intersection management," in *Proc. 10th Intell. Auton. Vehicles (IAV)*, Poland, Jan. 2019, pp. 233–238.
- [11] S. C. Ekpo, B. Adebisi, D. George, R. Kharel, and M. Uko, "System-level multicriteria modelling of payload operational times for communication satellite missions in LEO," *Recent Prog. Space Technol. Formerly, Recent Patents Space Technol.*, vol. 4, no. 1, pp. 67–77, Jun. 2014, doi: [10.2174/2210687104666140620221119](https://doi.org/10.2174/2210687104666140620221119).
- [12] H. Bagheri, M. Noor-A-Rahim, Z. Liu, H. Lee, D. Pesch, K. Moessner, and P. Xiao, "5G NR-V2X: Toward connected and cooperative autonomous driving," *IEEE Commun. Standards Mag.*, vol. 5, no. 1, pp. 48–54, Mar. 2021, doi: [10.1109/MCOMSTD.001.2000069](https://doi.org/10.1109/MCOMSTD.001.2000069).
- [13] R. W. Heath, Jr., "Vehicle-to-X communications: The killer application of millimeter wave," in *Proc. 1st ACM Workshop Millim.-Wave Netw. Sens. Syst.*, Oct. 2017, pp. 2–15, doi: [10.1145/3130242.3131489](https://doi.org/10.1145/3130242.3131489).
- [14] G. Hernandez-Oregon, M. E. Rivero-Angeles, J. C. Chimal-Eguía, A. Campos-Fentanes, J. G. Jimenez-Gallardo, U. O. Estevez-Alva, O. Juarez-Gonzalez, P. O. Rosas-Calderon, S. Sandoval-Reyes, and R. Menchaca-Mende, "Performance analysis of V2V and V2I LiFi communication systems in traffic lights," *Hindawi Wireless Commun. Mobile Comput.*, vol. 2019, p. 12, Aug. 2019, doi: [10.1155/2019/4279683](https://doi.org/10.1155/2019/4279683).
- [15] S. C. Ekpo and D. George, "A system engineering analysis of highly adaptive small satellites," *IEEE Syst. J.*, vol. 7, no. 4, pp. 642–648, Dec. 2013, doi: [10.1109/JSYST.2012.2198138](https://doi.org/10.1109/JSYST.2012.2198138).
- [16] J. I. Janjua, T. A. Khan, M. S. Khan, and M. Nadeem, "Li-fi communications in smart cities for truly connected vehicles," in *Proc. 2nd Int. Conf. Smart Cities, Autom. Intell. Comput. Syst. (ICON-SONICS)*, Oct. 2021, pp. 1–6, doi: [10.1109/ICON-SONICS53103.2021.9617200](https://doi.org/10.1109/ICON-SONICS53103.2021.9617200).
- [17] S. C. Ekpo and D. George, "Reconfigurable cooperative intelligent control design for space missions," *Recent Patents Space Technol.*, vol. 2, no. 1, pp. 2–11, Apr. 2012, doi: [10.2174/1877611611202010002](https://doi.org/10.2174/1877611611202010002).
- [18] I. Llatser, T. Michalke, M. Dolgov, F. Wildschutte, and H. Fuchs, "Cooperative automated driving use cases for 5G V2X communication," in *Proc. IEEE 2nd 5G World Forum (5GWF)*, Sep. 2019, pp. 120–125, doi: [10.1109/5GWF.2019.8911628](https://doi.org/10.1109/5GWF.2019.8911628).
- [19] M. Zafar, S. Ekpo, J. George, P. Sheedy, M. Uko, and A. Gibson, "Hybrid power divider and combiner for passive RFID tag wireless energy harvesting," *IEEE Access*, vol. 10, pp. 502–515, 2022, doi: [10.1109/ACCESS.2021.3138070](https://doi.org/10.1109/ACCESS.2021.3138070).
- [20] J. M. Mredith and M. Pope, *Summary of Rel-15 Work Items*, document TR 12.915, version 15.0.0, Release 15, 3GPP, 2019.
- [21] (2020). *PowerBroker2*. ELMDuino. [Online]. Available: <https://github.com/PowerBroker2/ELMDuino>
- [22] A. Salunke, A. Sharma, S. Bodake, and A. Chaurasia, "Inter-vehicular communication using Li-Fi technology to avoid the accident & sending emergency & help messages between vehicles using light," *Int. J. Res. Inf. Technol.*, vol. 1, no. 1, pp. 43–56, 2017.
- [23] M. Uko and S. Ekpo, "8–12 GHz pHEMT MMIC low-noise amplifier for 5G and fiber-integrated satellite applications," *Int. Rev. Aerosp. Eng.*, vol. 13, no. 3, pp. 99–107, 2020, doi: [10.15866/irease.v13i3.17998](https://doi.org/10.15866/irease.v13i3.17998).
- [24] S. Kulkarni, A. Darekar, and S. Shirol, "Proposed framework for V2V communication using Li-Fi technology," in *Proc. Int. Conf. Circuits, Controls, Commun. (CCUBE)*, Dec. 2017, pp. 187–190, doi: [10.1109/CCUBE.2017.8394163](https://doi.org/10.1109/CCUBE.2017.8394163).
- [25] R. Stuhlfauth, "Wireless communications for automotive applications," Rohde and Schwarz, Munich, Germany, White Paper, 2021.
- [26] V. Subbulakshmi, G. Prethija, B. Keerthana, R. Pavithra, and S. Kayathri, "Driver assistance system using Li-Fi technology based communication," Velammal Eng. College, Chennai, India, EasyChair Tech. Rep. 7380, Jan. 2017.
- [27] *Volkswagen and Siemens Make Crossroads Safer*, Volkswagen Newsroom, Wolfsburg, Germany, 2018.
- [28] S. Ekpo and D. George, "A deterministic multifunctional architecture for highly adaptive small satellites," *Int. J. Satell. Commun. Policy Manag.*, vol. 1, nos. 2–3, pp. 174–194, 2012, doi: [10.1504/IJSCPM.2012.049543](https://doi.org/10.1504/IJSCPM.2012.049543).
- [29] S. Yagaraya, S. F. A. Raza, A. Azman, M. F. A. Abdullah, and A. S. M. Supian, "Light fidelity (Li-Fi) for vehicular communication: A comprehensive study," *J. Telecommun., Electron. Comput. Eng.*, vol. 13, no. 3, pp. 13–17, Sep. 2021.
- [30] H. Zhou, W. Xu, J. Chen, and W. Wang, "Evolutionary V2X technologies toward the Internet of Vehicles: Challenges and opportunities," *Proc. IEEE*, vol. 108, no. 2, pp. 308–323, Feb. 2020, doi: [10.1109/JPROC.2019.2961937](https://doi.org/10.1109/JPROC.2019.2961937).
- [31] S. C. Ekpo and D. George, "Impact of noise figure on a satellite link performance," *IEEE Commun. Lett.*, vol. 15, no. 9, pp. 977–979, Sep. 2011, doi: [10.1109/LCOMM.2011.072011.111073](https://doi.org/10.1109/LCOMM.2011.072011.111073).
- [32] I. Tavakkolnia, D. Cheadle, R. Bian, T. H. Loh, and H. Haas, "High speed millimeter-wave and visible light communication with off-the-shelf components," in *Proc. IEEE Globecom Workshops (GC Wkshps)*, Dec. 2020, pp. 1–6, doi: [10.1109/GCWkshps50303.2020.9367475](https://doi.org/10.1109/GCWkshps50303.2020.9367475).
- [33] R. Bian, I. Tavakkolnia, and H. Haas, "15.73 Gb/s visible light communication with off-the-shelf LEDs," *J. Lightw. Technol.*, vol. 37, no. 10, pp. 2418–2424, May 15, 2019, doi: [10.1109/JLT.2019.2906464](https://doi.org/10.1109/JLT.2019.2906464).
- [34] A. M. Nor, "Access point selection in beyond 5G hybrid MmWave/Wi-Fi/Li-Fi network," *Phys. Commun.*, vol. 46, Jun. 2021, Art. no. 101299, doi: [10.1016/j.phycom.2021.101299](https://doi.org/10.1016/j.phycom.2021.101299).
- [35] X. Wu and D. C. O'Brien, "Parallel transmission LiFi," *IEEE Trans. Wireless Commun.*, vol. 19, no. 10, pp. 6268–6276, Oct. 2020, doi: [10.1109/TWC.2020.3001983](https://doi.org/10.1109/TWC.2020.3001983).
- [36] Highways Agency and Driver and Vehicles Standards Agency. (May 2014). *Highways Agency warns Tailgaters That 'Only a Fool Breaks the 2-Second Rule'*. Accessed: Jan. 25, 2023. [Online]. Available: <https://www.gov.uk/government/news/highways-agency-warns-tailgaters-that-only-a-fool-breaks-the-two-second-rule>
- [37] B. Groza and P. S. Murvay, "Higher layer authentication for broadcast in controller area networks," in *Proc. Int. Conf. Secur. Cryptogr.*, Jul. 2011, pp. 188–197.
- [38] I. I. M. A. Sulayman, R. He, M. Manka, A. Ning, and A. Ouda, "LiFi/WiFi authentication and handover protocols: Survey, evaluation, and recommendation," in *Proc. Int. Symp. Netw., Comput. Commun. (ISNCC)*, Dubai, United Arab Emirates, Oct. 2021, pp. 1–6, doi: [10.1109/ISNCC52172.2021.9615853](https://doi.org/10.1109/ISNCC52172.2021.9615853).



IAIN LAU received the B.Eng. degree (Hons.) in electrical and electronic engineering from Manchester Metropolitan University, Manchester, U.K., in May 2022, where he is currently pursuing the Ph.D. degree in engineering. His research interests include free-space optical communication, radio-frequency millimeter-wave communications, autonomous vehicles, and vehicle-to-everything communication.



SUNDAY EKPO (Senior Member, IEEE) received the M.Sc. degree in communication engineering from the University of Manchester, Manchester, U.K., in September 2008, the Ph.D. degree in electrical and electronic engineering from the University of Manchester, and the M.A. degree in higher education. He holds a PGC in academic practice. He is a Senior Lecturer of electrical and electronic engineering with Manchester Metropolitan University, U.K., where he leads the Communication and Space Systems Engineering Research Team. He is also a Board of Studies International Expert with M.Tech. Communication Systems Program, Amrita Vishwa Vidyapeetham University, Coimbatore Campus, India. He specializes in energy- and spectrum-efficient highly adaptive satellite system design; multi-physics design and modeling of RF, microwave, millimeter-wave, and optical transceivers; the Internet of Things sensors characterization; and multi-objective systems engineering. He was a recipient of the Huawei's Influential Thinkers in Engineering and Technology Recognition, in 2019. He is a member of the U.K. Research and Innovation Talent Panel College; Engineering and Physical Sciences Research Council Peer-Review College; Institution of Engineering and Technology, U.K., and the American Institute of Aeronautics and Astronautics. He is a Chartered Engineer and a Senior Fellow of the Higher Education Academy, U.K.



MUAZZAM ZAFAR received the B.Eng. degree in electrical/electronics engineering from the COM-SATS Institute of Information and Technology, Abbottabad, Pakistan, and the M.Sc. degree (Hons.) in electronics engineering from Manchester Metropolitan University, Manchester, U.K., in September 2019, where he is currently pursuing the M.Res. degree in communication engineering. His research interests include RF energy harvesting for 5G communication applications, the

Internet of Things (IoT) sensor characterization, antenna modeling, and RF transceiver characterization.



MUHAMMAD IJAZ (Member, IEEE) received the M.Sc. degree in optoelectronic and communication engineering and the Ph.D. degree in free-space optical (FSO) communications from Northumbria University, Newcastle upon Tyne, U.K., in 2009 and 2013, respectively. He was a Research Fellow in visible light communication/Li-Fi with the University of Edinburgh, U.K., from 2013 to 2015. He is currently a Lead International and a Senior Lecturer with

the Department of Engineering, Manchester Metropolitan University, U.K. He is also leading the Laser and Optics Communication (LOC) Laboratory. He has been working with a number of industries, technopreneurs, and on two knowledge transfer partnership projects in the areas of embedded systems, the IoT, cloud communication networks, digital signal processing, and smart sensors designs. He was awarded Northumbria University Studentship to pursue his Ph.D. degree. He has secured more than £500,000 funding. He has published over 75 peer-reviewed articles in the area of optical wireless communications and sensor design and has been cited more than 1100 times. His research interests include optical wireless/fiber communications networks for cyber-physical systems and advanced modulation schemes, including OFDM, visible light communication, applications of Li-Fi, power line communications, the IoTs and photonics, and optical sensors design. He is a member of IET.



ANDY GIBSON received the D.Sc. degree in microwave engineering and technology. He is a research expertise in high power circuits for radar systems, for over 25 years. Prior to his post as a Pro-Vice-Chancellor of science and engineering, he was the first Head of the School of Electrical and Electronic Engineering and then the Head of the School of Mechanical, Aerospace and Civil Engineering, University of Manchester. He was also responsible for Tyndall Manchester, a Rolls-

Royce Technology Centre, a Project Management Professional Development Group, and the EDF Modeling and Simulation Centre. He has gained international recognition for the application of multiphysics finite element techniques to high power, non-linear, and non-reciprocal ferrite components. He has published a research on electronic waste with Manchester Business School. His research interest includes re-manufacturing as applied to electrical and electronic equipment. He has chaired a major international conference in microwave technology in London. He is extremely passionate about science and engineering, particularly in the city of Manchester, and very excited about building world-class partnerships, excellence in education, scholarship, and research across the breadth of STEM disciplines. He continues to be involved with teaching in electronic circuits and is a keen exponent of sustainable energy, commuting by bicycle everyday into Manchester from Altrincham.

...